

Understanding individual human mobility patterns

Marta C. González,^{1,2} César A. Hidalgo,¹ and Albert-László Barabási^{1,2,3}

¹*Center for Complex Network Research and Department of Physics and Computer Science,
University of Notre Dame, Notre Dame IN 46556.*

²*Center for Complex Network Research and Department of Physics,
Biology and Computer Science, Northeastern University, Boston MA 02115.*

³*Center for Cancer Systems Biology, Dana Farber Cancer Institute, Boston, MA 02115.*

(Dated: November 26, 2024)

Despite their importance for urban planning [1], traffic forecasting [2], and the spread of biological [3, 4, 5] and mobile viruses [6], our understanding of the basic laws governing human motion remains limited thanks to the lack of tools to monitor the time resolved location of individuals. Here we study the trajectory of 100,000 anonymized mobile phone users whose position is tracked for a six month period. We find that in contrast with the random trajectories predicted by the prevailing Lévy flight and random walk models [7], human trajectories show a high degree of temporal and spatial regularity, each individual being characterized by a time independent characteristic length scale and a significant probability to return to a few highly frequented locations. After correcting for differences in travel distances and the inherent anisotropy of each trajectory, the individual travel patterns collapse into a single spatial probability distribution, indicating that despite the diversity of their travel history, humans follow simple reproducible patterns. This inherent similarity in travel patterns could impact all phenomena driven by human mobility, from epidemic prevention to emergency response, urban planning and agent based modeling.

Given the many unknown factors that influence a population's mobility patterns, ranging from means of transportation to job and family imposed restrictions and priorities, human trajectories are often approximated with various random walk or diffusion models [7, 8]. Indeed, early measurements on albatrosses, bumblebees, deer and monkeys [9, 10] and more recent ones on marine predators [11] suggested that animal trajectory is approximated by a Lévy flight [12, 13], a random walk whose step size Δr follows a power-law distribution $P(\Delta r) \sim \Delta r^{-(1+\beta)}$ with $\beta < 2$. While the Lévy statistics for some animals require further study [14], Brockmann *et al.* [7] generalized this finding to humans, documenting that the distribution of distances between consecutive sight-

ings of nearly half-million bank notes is fat tailed. Given that money is carried by individuals, bank note dispersal is a proxy for human movement, suggesting that human trajectories are best modeled as a continuous time random walk with fat tailed displacements and waiting time distributions [7]. A particle following a Lévy flight has a significant probability to travel very long distances in a single step [12, 13], which appears to be consistent with human travel patterns: most of the time we travel only over short distances, between home and work, while occasionally we take longer trips.

Each consecutive sightings of a bank note reflects the composite motion of two or more individuals, who owned the bill between two reported sightings. Thus it is not clear if the observed distribution reflects the motion of individual users, or some hitherto unknown convolution between population based heterogeneities and individual human trajectories. Contrary to bank notes, mobile phones are carried by the same individual during his/her daily routine, offering the best proxy to capture individual human trajectories [15, 16, 17, 18, 19].

We used two data sets to explore the mobility pattern of individuals. The first (D_1) consists of the mobility patterns recorded over a six month period for 100,000 individuals selected randomly from a sample of over 6 million anonymized mobile phone users. Each time a user initiates or receives a call or SMS, the location of the tower routing the communication is recorded, allowing us to reconstruct the user's time resolved trajectory (Figs. 1a and b). The time between consecutive calls follows a bursty pattern [20] (see Fig. S1 in the SM), indicating that while most consecutive calls are placed soon after a previous call, occasionally there are long periods without any call activity. To make sure that the obtained results are not affected by the irregular call pattern, we also study a data set (D_2) that captures the location of 206 mobile phone users, recorded every two hours for an entire week. In both datasets the spatial resolution is determined by the local density of the more than 10^4 mobile towers, registering movement only when the user moves between areas serviced by different towers. The average service area of each tower is approximately 3 km^2 and over 30% of the towers cover an area of 1 km^2 or less.

To explore the statistical properties of the population's mobility patterns we measured the distance between user's positions at consecutive calls, capturing 16,264,308 displacements for the D_1 and 10,407 displacements for the D_2 datasets. We find that the distribution of displacements over all users is well approximated by a truncated power-law

$$P(\Delta r) = (\Delta r + \Delta r_0)^{-\beta} \exp(-\Delta r/\kappa), \quad (1)$$

with $\beta = 1.75 \pm 0.15$, $\Delta r_0 = 1.5$ km and cutoff values $\kappa|_{D_1} = 400$ km, and $\kappa|_{D_2} = 80$ km (Fig. 1c, see the SM for statistical validation). Note that the observed scaling exponent is not far from $\beta_B = 1.59$ observed in Ref. [7] for bank note dispersal, suggesting that the two distributions may capture the same fundamental mechanism driving human mobility patterns.

Equation (1) suggests that human motion follows a truncated Lévy flight [7]. Yet, the observed shape of $P(\Delta r)$ could be explained by three distinct hypotheses: A. Each individual follows a Lévy trajectory with jump size distribution given by (1). B. The observed distribution captures a population based heterogeneity, corresponding to the inherent differences between individuals. C. A population based heterogeneity coexists with individual Lévy trajectories, hence (1) represents a convolution of hypothesis A and B.

To distinguish between hypotheses A, B and C we calculated the radius of gyration for each user (see Methods), interpreted as the typical distance traveled by user a when observed up to time t (Fig. 1b). Next, we determined the radius of gyration distribution $P(r_g)$ by calculating r_g for all users in samples D_1 and D_2 , finding that they also can be approximated with a truncated power-law

$$P(r_g) = (r_g + r_g^0)^{-\beta_r} \exp(-r_g/\kappa), \quad (2)$$

with $r_g^0 = 5.8$ km, $\beta_r = 1.65 \pm 0.15$ and $\kappa = 350$ km (Fig. 1d, see SM for statistical validation). Lévy flights are characterized by a high degree of intrinsic heterogeneity, raising the possibility that (2) could emerge from an ensemble of identical agents, each following a Lévy trajectory. Therefore, we determined $P(r_g)$ for an ensemble of agents following a Random Walk (RW), Lévy-Flight (LF) or Truncated Lévy-Flight (TLF) (Figure 1d) [8, 12, 13]. We find that an ensemble of Lévy agents display a significant degree of heterogeneity in r_g , yet is not sufficient to explain the truncated power law distribution $P(r_g)$ exhibited by the mobile phone users. Taken together, Figs. 1c and d suggest that the difference in the range of typical mobility patterns of individuals (r_g) has a strong impact on the truncated Lévy behavior seen in (1), ruling out hypothesis A.

If individual trajectories are described by a LF or TLF , then the radius of gyration should increase in time as $r_g(t) \sim t^{3/(2+\beta)}$ [21, 22] while for a RW $r_g(t) \sim t^{1/2}$. That is, the longer we observe a user, the higher the chances that she/he will travel to areas not visited before. To check the validity of these predictions we measured the time dependence of the radius of gyration for users whose gyration radius would be considered small ($r_g(T) \leq 3$ km), medium ($20 < r_g(T) \leq 30$ km) or large ($r_g(T) > 100$ km) at the end of our observation period ($T = 6$ months). The

results indicate that the time dependence of the average radius of gyration of mobile phone users is better approximated by a logarithmic increase, not only a manifestly slower dependence than the one predicted by a power law, but one that may appear similar to a saturation process (Fig. 2a and Fig. S4).

In Fig. 2b, we have chosen users with similar asymptotic $r_g(T)$ after $T = 6$ months, and measured the jump size distribution $P(\Delta r|r_g)$ for each group. As the inset of Fig. 2b shows, users with small r_g travel mostly over small distances, whereas those with large r_g tend to display a combination of many small and a few larger jump sizes. Once we rescale the distributions with r_g (Fig. 2b), we find that the data collapses into a single curve, suggesting that a single jump size distribution characterizes all users, independent of their r_g . This indicates that $P(\Delta r|r_g) \sim r_g^{-\alpha} F(\Delta r/r_g)$, where $\alpha \approx 1.2 \pm 0.1$ and $F(x)$ is an r_g independent function with asymptotic behavior $F(x < 1) \sim x^{-\alpha}$ and rapidly decreasing for $x \gg 1$. Therefore the travel patterns of individual users may be approximated by a Lévy flight up to a distance characterized by r_g . Most important, however, is the fact that the individual trajectories are bounded beyond r_g , thus large displacements which are the source of the distinct and anomalous nature of Lévy flights, are statistically absent. To understand the relationship between the different exponents, we note that the measured probability distributions are related by $P(\Delta r) = \int_0^\infty P(\Delta r|r_g)P(r_g)dr_g$, which suggests (see SM) that up to the leading order we have $\beta = \beta_r + \alpha - 1$, consistent, within error bars, with the measured exponents. This indicates that the observed jump size distribution $P(\Delta r)$ is in fact the convolution between the statistics of individual trajectories $P(\Delta r_g|r_g)$ and the population heterogeneity $P(r_g)$, consistent with hypothesis C.

To uncover the mechanism stabilizing r_g we measured the return probability for each individual $F_{pt}(t)$ [22], defined as the probability that a user returns to the position where it was first observed after t hours (Fig. 2c). For a two dimensional random walk $F_{pt}(t)$ should follow $\sim 1/(t \ln(t)^2)$ [22]. In contrast, we find that the return probability is characterized by several peaks at 24 h, 48 h, and 72 h, capturing a strong tendency of humans to return to locations they visited before, describing the recurrence and temporal periodicity inherent to human mobility [23, 24].

To explore if individuals return to the same location over and over, we ranked each location based on the number of times an individual was recorded in its vicinity, such that a location with $L = 3$ represents the third most visited location for the selected individual. We find that the probability of finding a user at a location with a given rank L is well approximated by $P(L) \sim 1/L$, independent of the number of locations visited by the user (Fig. 2d). Therefore people devote most

of their time to a few locations, while spending their remaining time in 5 to 50 places, visited with diminished regularity. Therefore, the observed logarithmic saturation of $r_g(t)$ is rooted in the high degree of regularity in their daily travel patterns, captured by the high return probabilities (Fig. 2b) to a few highly frequented locations (Fig. 2d).

An important quantity for modeling human mobility patterns is the probability $\Phi_a(x, y)$ to find an individual a in a given position (x, y) . As it is evident from Fig. 1b, individuals live and travel in different regions, yet each user can be assigned to a well defined area, defined by home and workplace, where she or he can be found most of the time. We can compare the trajectories of different users by diagonalizing each trajectory's inertia tensor, providing the probability of finding a user in a given position (see Fig. 3a) in the user's intrinsic reference frame (see SM for the details). A striking feature of $\Phi(x, y)$ is its prominent spatial anisotropy in this intrinsic reference frame (note the different scales in Fig 3a), and we find that the larger an individual's r_g the more pronounced is this anisotropy. To quantify this effect we defined the anisotropy ratio $S \equiv \sigma_y/\sigma_x$, where σ_x and σ_y represent the standard deviation of the trajectory measured in the user's intrinsic reference frame (see SM). We find that S decreases monotonically with r_g (Fig. 3c), being well approximated with $S \sim r_g^{-\eta}$, for $\eta \approx 0.12$. Given the small value of the scaling exponent, other functional forms may offer an equally good fit, thus mechanistic models are required to identify if this represents a true scaling law, or only a reasonable approximation to the data.

To compare the trajectories of different users we remove the individual anisotropies, rescaling each user trajectory with its respective σ_x and σ_y . The rescaled $\tilde{\Phi}(x/\sigma_x, y/\sigma_y)$ distribution (Fig. 3b) is similar for groups of users with considerably different r_g , *i.e.*, after the anisotropy and the r_g dependence is removed all individuals appear to follow the same universal $\tilde{\Phi}(\tilde{x}, \tilde{y})$ probability distribution. This is particularly evident in Fig. 3d, where we show the cross section of $\tilde{\Phi}(x/\sigma_x, 0)$ for the three groups of users, finding that apart from the noise in the data the curves are indistinguishable.

Taken together, our results suggest that the Lévy statistics observed in bank note measurements capture a convolution of the population heterogeneity (2) and the motion of individual users. Individuals display significant regularity, as they return to a few highly frequented locations, like home or work. This regularity does not apply to the bank notes: a bill always follows the trajectory of its current owner, *i.e.* dollar bills diffuse, but humans do not.

The fact that individual trajectories are characterized by the same r_g -independent two dimensional probability distribution $\tilde{\Phi}(x/\sigma_x, y/\sigma_y)$ suggests that key statistical characteristics of indi-

vidual trajectories are largely indistinguishable after rescaling. Therefore, our results establish the basic ingredients of realistic agent based models, requiring us to place users in number proportional with the population density of a given region and assign each user an r_g taken from the observed $P(r_g)$ distribution. Using the predicted anisotropic rescaling, combined with the density function $\tilde{\Phi}(x, y)$, whose shape is provided as Table 1 in the SM, we can obtain the likelihood of finding a user in any location. Given the known correlations between spatial proximity and social links, our results could help quantify the role of space in network development and evolution [25, 26, 27, 28, 29] and improve our understanding of diffusion processes [8, 30].

We thank D. Brockmann, T. Geisel, J. Park, S. Redner, Z. Toroczkai and P. Wang for discussions and comments on the manuscript. This work was supported by the James S. McDonnell Foundation 21st Century Initiative in Studying Complex Systems, the National Science Foundation within the DDDAS (CNS-0540348), ITR (DMR-0426737) and IIS-0513650 programs, and the U.S. Office of Naval Research Award N00014-07-C. Data analysis was performed on the Notre Dame Biocomplexity Cluster supported in part by NSF MRI Grant No. DBI-0420980. C.A. Hidalgo acknowledges support from the Kellogg Institute at Notre Dame.

Supplementary Information is linked to the online version of the paper at www.nature.com/nature.

Author Information Correspondence and requests for materials should be addressed to A.-L.B. (e-mail: alb@nd.edu)

-
- [1] Horner, M.W. & O’Kelly, M.E.S Embedding economies of scale concepts for hub networks design. *Journal of Transportation Geography* **9**, 255-265 (2001).
 - [2] Kitamura, R., Chen, C., Pendyala, R.M. & Narayanan, R. Micro-simulation of daily activity-travel patterns for travel demand forecasting. *Transportation* **27**, 25-51 (2000).
 - [3] Colizza, V., Barrat, A., Barthélemy, M., Valleron, A.-J. & Vespignani, A. Modeling the Worldwide Spread of Pandemic Influenza: Baseline Case and Containment Interventions. *PLoS Medicine* **4**, 095-0110 (2007).
 - [4] Eubank, S., Guclu, H., Kumar, V.S.A., Marathe, M.V., Srinivasan, A., Toroczkai, Z. & Wang, N. Controlling Epidemics in Realistic Urban Social Networks. *Nature* **429**, 180 (2004).
 - [5] Hufnagel, L., Brockmann, D. & Geisel, T. Forecast and control of epidemics in a globalized world. *Proceedings of the National Academy of Sciences of the United States of America* **101**, 15124-15129 (2004).
 - [6] Kleinberg, J. The wireless epidemic. *Nature* **449**, 287-288 (2007).
 - [7] D. Brockmann, D., Hufnagel, L. & Geisel, T. The scaling laws of human travel. *Nature* **439**, 462-465 (2006).
 - [8] Havlin, S. & ben-Avraham, D. Diffusion in Disordered Media. *Advances in Physics* **51**, 187-292 (2002).
 - [9] Viswanathan, G.M., Afanasyev, V., Buldyrev, S.V., Murphy, E.J., Prince, P.A. & Stanley, H.E. Lévy Flight Search Patterns of Wandering Albatrosses. *Nature* **381**, 413-415 (1996).
 - [10] Ramos-Fernandez, G., Mateos, J.L., Miramontes, O., Cocho, G., Larralde, H. & Ayala-Orozco, B., Lévy walk patterns in the foraging movements of spider monkeys (*Ateles geoffroyi*). *Behavioral ecology and Sociobiology* **55**, 223-230 (2004).
 - [11] Sims D.W. *et al.* Scaling laws of marine predator search behaviour. *Nature* **451**, 1098-1102 (2008).
 - [12] Klafter, J., Shlesinger, M.F. & Zumofen, G. Beyond Brownian Motion. *Physics Today* **49**, 33-39 (1996).
 - [13] Mantegna, R.N. & Stanley, H.E. Stochastic Process with Ultraslow Convergence to a Gaussian: The Truncated Lévy Flight. *Physical Review Letters* **73**, 2946-2949 (1994).
 - [14] Edwards, A.M., Phillips, R.A., Watkins, N.W., Freeman, M.P., Murphy, E.J., Afanasyev, V., Buldyrev, S.V., da Luz, M.G.E., Raposo, E. P., Stanley, H. E. & Viswanathan, G. M. Revisiting Lévy flight

- search patterns of wandering albatrosses, bumblebees and deer. *Nature* **449**, 1044-1049 (2007).
- [15] Sohn, T., Varshavsky, A., LaMarca, A., Chen, M.Y., Choudhury, T., Smith, I., Consolvo, S., Hightower, J., Griswold, W.G. & de Lara, E. *Lecture Notes in Computer Sciences: Proc. 8th International Conference UbiComp 2006*. (Springer, Berlin, 2006).
- [16] Onnela, J.-P., Saramäki, J., Hyvönen, J., Szabó, G., Lazer, D., Kaski, K., Kertész, K. & Barabási A.L. Structure and tie strengths in mobile communication networks. *Proceedings of the National Academy of Sciences of the United States of America* **104**, 7332-7336 (2007).
- [17] González, M.C. & Barabási, A.-L. Complex networks: From data to models. *Nature Physics* **3**, 224-225 (2007).
- [18] Palla, G., Barabási, A.-L. & Vicsek, T. Quantifying social group evolution. *Nature* **446**, 664-667 (2007).
- [19] Hidalgo C.A. & Rodriguez-Sickert C. The dynamics of a mobile phone network. *Physica A* **387**, 3017-30224.
- [20] Barabási, A.-L. The origin of bursts and heavy tails in human dynamics. *Nature* **435**, 207-211 (2005).
- [21] Hughes, B.D. *Random Walks and Random Environments*. (Oxford University Press, USA, 1995).
- [22] Redner, S. *A Guide to First-Passage Processes*. (Cambridge University Press, UK, 2001).
- [23] Schlich, R. & Axhausen, K. W. Habitual travel behaviour: Evidence from a six-week travel diary. *Transportation* **30**, 13-36 (2003).
- [24] Eagle, N. & Pentland, A. Eigenbehaviours: Identifying Structure in Routine. *submitted to Behavioral Ecology and Sociobiology* (2007).
- [25] Yook, S.-H., Jeong, H. & Barabási A.L. Modeling the Internet's large-scale topology. *Proceedings of the Nat'l Academy of Sciences* **99**, 13382-13386 (2002).
- [26] Caldarelli, G. *Scale-Free Networks: Complex Webs in Nature and Technology*. (Oxford University Press, USA, 2007).
- [27] Dorogovtsev, S.N. & Mendes, J.F.F. *Evolution of Networks: From Biological Nets to the Internet and WWW*. (Oxford University Press, USA, 2003).
- [28] Song C.M., Havlin S. & Makse H.A. Self-similarity of complex networks. *Nature* **433**, 392-395 (2005).
- [29] González, M.C., Lind, P.G. & Herrmann, H.J. A system of mobile agents to model social networks. *Physical Review Letters* **96**, 088702 (2006).
- [30] Cecconi, F., Marsili, M., Banavar, J.R. & Maritan, A. Diffusion, peer pressure, and tailed distributions.

Physical Review Letters **89**, 088102 (2002).

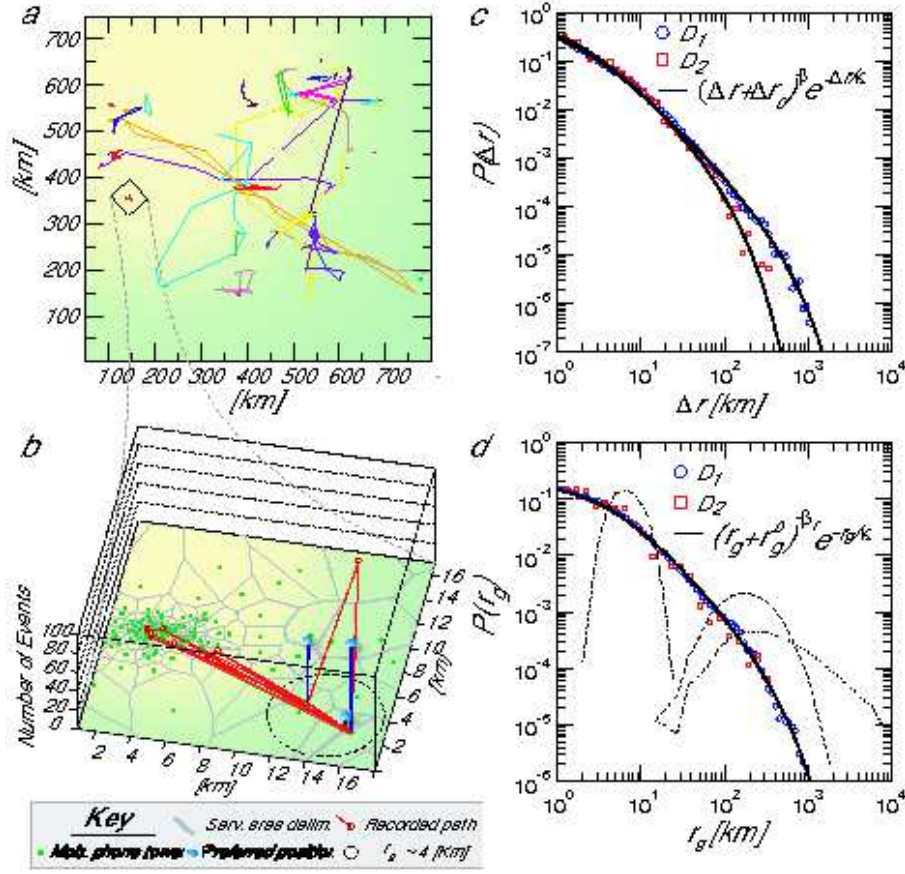


FIG. 1: Basic human mobility patterns. **a**, Week-long trajectory of 40 mobile phone users indicate that most individuals travel only over short distances, but a few regularly move over hundreds of kilometers. Panel **b**, displays the detailed trajectory of a single user. The different phone towers are shown as green dots, and the Voronoi lattice in grey marks the approximate reception area of each tower. The dataset studied by us records only the identity of the closest tower to a mobile user, thus we can not identify the position of a user within a Voronoi cell. The trajectory of the user shown in **b** is constructed from 186 two hourly reports, during which the user visited a total of 12 different locations (tower vicinities). Among these, the user is found 96 and 67 occasions in the two most preferred locations, the frequency of visits for each location being shown as a vertical bar. The circle represents the radius of gyration centered in the trajectory's center of mass. **c**, Probability density function $P(\Delta r)$ of travel distances obtained for the two studied datasets D_1 and D_2 . The solid line indicates a truncated power law whose parameters are provided in the text (see Eq. 1). **d**, The distribution $P(r_g)$ of the radius of gyration measured for the users, where $r_g(T)$ was measured after $T = 6$ months of observation. The solid line represent a similar truncated power law fit (see Eq. 2). The dotted, dashed and dot-dashed curves show $P(r_g)$ obtained from the standard null models (RW, LF and TLF), where for the TLF we used the same step size distribution as the one measured for the mobile phone users.

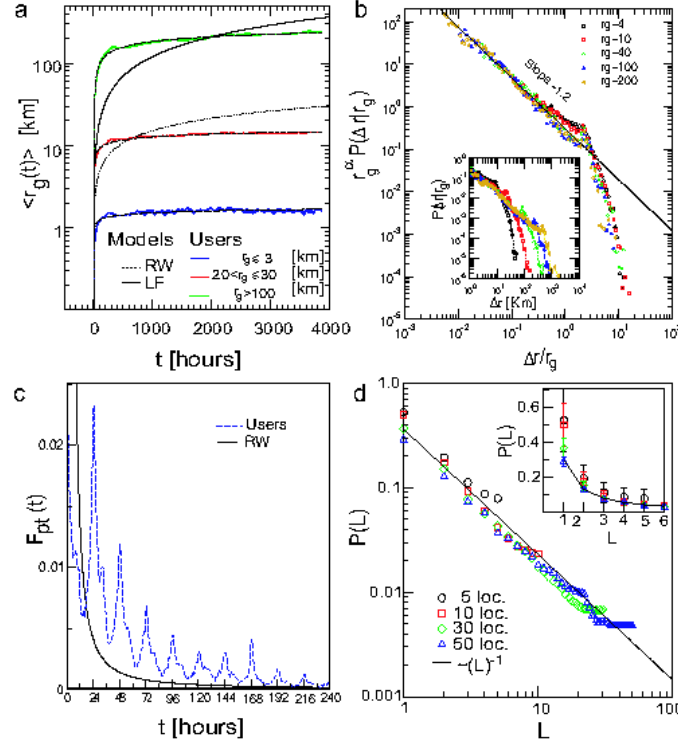


FIG. 2: The bounded nature of human trajectories. **a**, Radius of gyration, $\langle r_g(t) \rangle$ vs time for mobile phone users separated in three groups according to their final $r_g(T)$, where $T = 6$ months. The black curves correspond to the analytical predictions for the random walk models, increasing in time as $\langle r_g(t) \rangle|_{LF,TLF} \sim t^{3/2+\beta}$ (solid), and $\langle r_g(t) \rangle|_{RW} \sim t^{0.5}$ (dotted). The dashed curves corresponding to a logarithmic fit of the form $A+B \ln(t)$, where A and B depend on r_g . **b**, Probability density function of individual travel distances $P(\Delta r|r_g)$ for users with $r_g = 4, 10, 40, 100$ and 200 km. As the inset shows, each group displays a quite different $P(\Delta r|r_g)$ distribution. After rescaling the distance and the distribution with r_g (main panel), the different curves collapse. The solid line (power law) is shown as a guide to the eye. **c**, Return probability distribution, $F_{pt}(t)$. The prominent peaks capture the tendency of humans to regularly return to the locations they visited before, in contrast with the smooth asymptotic behavior $\sim 1/(t \ln(t)^2)$ (solid line) predicted for random walks. **d**, A Zipf plot showing the frequency of visiting different locations. The symbols correspond to users that have been observed to visit $n_L = 5, 10, 30$, and 50 different locations. Denoting with (L) the rank of the location listed in the order of the visit frequency, the data is well approximated by $R(L) \sim L^{-1}$. The inset is the same plot in linear scale, illustrating that 40% of the time individuals are found at their first two preferred locations.

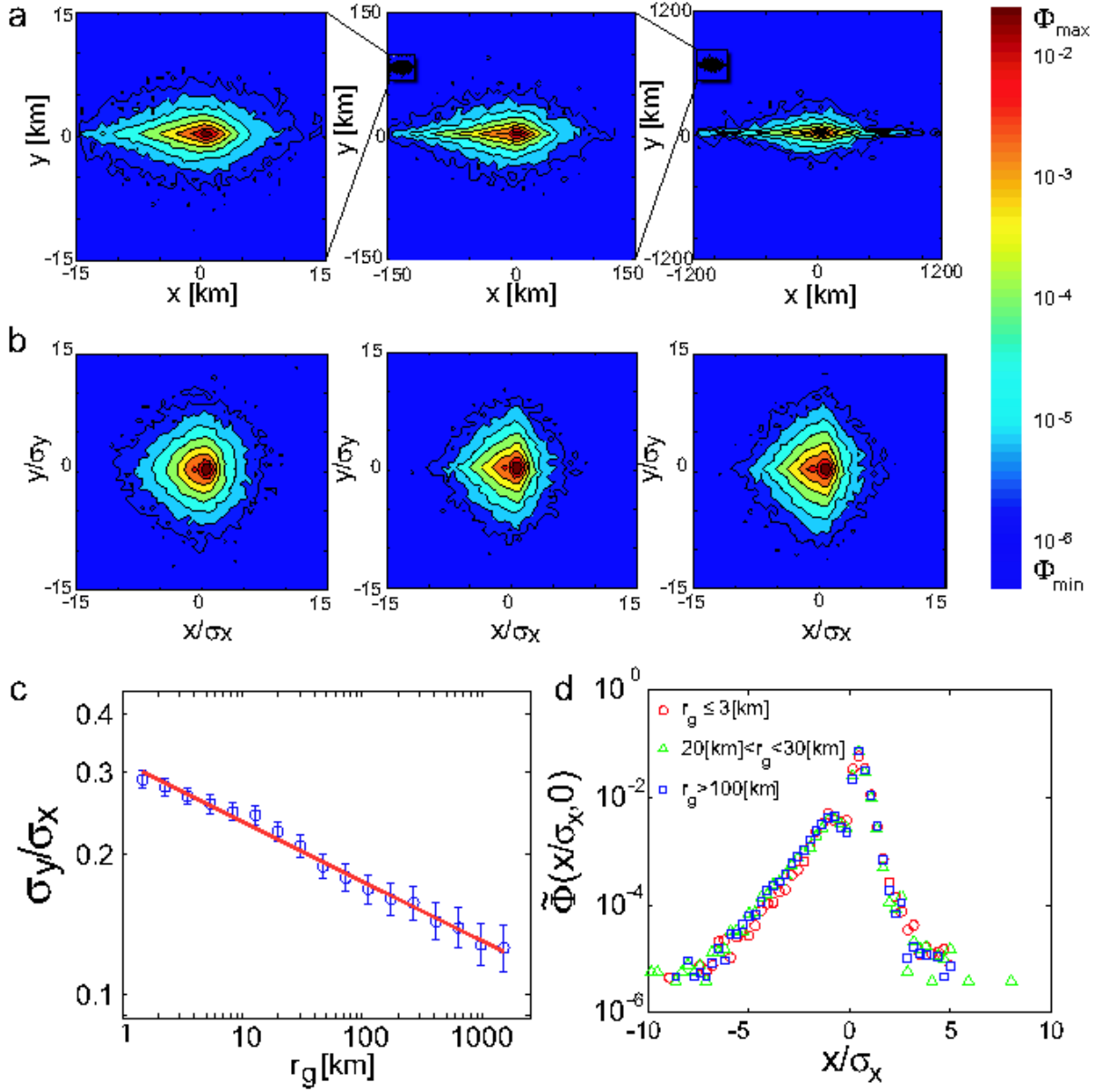


FIG. 3: The shape of human trajectories. **a**, The probability density function $\Phi(x, y)$ of finding a mobile phone user in a location (x, y) in the user's intrinsic reference frame (see SM for details). The three plots, from left to right, were generated for 10,000 users with: $r_g \leq 3$, $20 < r_g \leq 30$ and $r_g > 100$ km. The trajectories become more anisotropic as r_g increases. **b**, After scaling each position with σ_x and σ_y the resulting $\tilde{\Phi}(x/\sigma_x, y/\sigma_y)$ has approximately the same shape for each group. **c**, The change in the shape of $\Phi(x, y)$ can be quantified calculating the isotropy ratio $S \equiv \sigma_y/\sigma_x$ as a function of r_g , which decreases as $S \sim r_g^{-0.12}$ (solid line). Error bars represent the standard error. **d**, $\tilde{\Phi}(x/\sigma_x, 0)$ representing the x-axis cross section of the rescaled distribution $\tilde{\Phi}(x/\sigma_x, y/\sigma_y)$ shown in b.